INSTITUTE OF PHYSICS PUBLISHING PLASMA SOURCES SCIENCE AND TECHNOLOGY

Plasma Sources Sci. Technol. **13** (2004) 127–134 PII: S0963-0252(04)71848-4

Non-stationary charging of a dust grain in decaying streamer-channel plasma

N Yu Babaeva[1], J K Lee[2] and H C Kim[1]

Department of Electronic and Electrical Engineering, Pohang University of Science and Technology, Pohang 790-784, Korea

E-mail: jkl@postech.ac.kr

Received 2 February 2003
Published 15 December 2003
Online at stacks.iop.org/PSST/13/127 (DOI: 10.1088/0963-0252/13/1/016)

Abstract

The process of a dust grain charging in non-stationary (decaying) air plasma in external electric fields typical of a streamer channel at atmospheric air pressure is investigated numerically using two-dimensional spherical coordinates. The characteristic timescale on which the grain acquires maximal electric charge is found to be determined by the rate of electron attachment. For zero external field, the process of charging in decaying air plasma is compared with the analogous process in nitrogen (non-attaching gas). For non-zero external electric fields in air plasma, the correlation between the charging time and the field dependence of the attachment rate is revealed. For high values of external electric fields, a streamer discharge starting from the dust grain is observed, analogous to Trichel pulses in a negative corona.

1. Introduction

Streamer (corona) discharges were described in the 1940s by Loeb [1] and Meek [2] and are still under investigation today. They are an effective tool for various plasma chemical applications such as ozone generation from air and oxygen and removal of toxic agents from flue gases and polluted air [3]. At present one of the most important scientific questions that remain is quantitative modelling of corona discharges, accounting for dust particles or aerosols.

The physics of dusty plasmas has attracted considerable attention from the viewpoint of both basic plasma physics and plasma applications (see [4–8] and references therein). The greatest interest in research on these plasmas has arisen in recent years in connection with the rapid development of microtechnologies and technologies for producing new materials in plasma reactors. Many theoretical studies have addressed various questions such as particle formation and charging [9, 10]. The presence of dust grains in a plasma can greatly modify its properties. In gas-insulated systems, they can reduce the breakdown voltage. When the dust grain density is sufficiently high, this can lead to electron depletion in the quasi-neutral dusty plasma and can affect the streamer-channel conductivity. Dust charging can also provide opportunities. Large commercial electrostatic precipitators with pulsed feeding voltage utilize corona discharges for charging the dust particles [11, 12]. A study of the electric charge accumulated on the particles enables us to carry out an analysis of their mobility or movement in an electric field in order to control the particle trajectories in several electrostatic technologies including air cleaning, electrostatic separators, electrostatic coating and printing.

Owing to the high mobility of electrons, non-emitting dust particles acquire an equilibrium negative charge matching with the parameters of the surrounding plasma. However, the charge may be a function of time and position of the particle in plasma with varying parameters. In this study, we aim at modelling the process of a dust grain charging in non-stationary (decaying) air plasmas of the streamer channel. This problem has been little studied as most papers deal with the charging process in stationary plasmas.

2. Basic features of the streamer structure

The basic features of the streamer structure are demonstrated in figures 1 and 2, where the profiles of the absolute values of the electric field and electron number density along the streamer axis are presented calculated according to the model developed in [13, 14]. The streamer is a thin cylindrical

[1] Permanent address: Institute for High Temperatures, Russian Academy of Sciences, Moscow 127412, Russia

[2] Author to whom any correspondence should be addressed.

conducting channel, which can be divided into a very narrow frontal zone or head and a channel connecting the head with electrodes. In the head the electric field, E_h, is high, and ionization of gas molecules occurs. The channel is a passive region of weakly ionized plasma through which conduction current flows while a pulse of external voltage is applied. In the channel electric field, E_{ch}, the electron density and other parameters vary relatively slow. The plasma in the inner part of the channel is quasi-neutral, and space charge is concentrated at the boundary. The radial component of the electric field inside the channel is almost zero.

The streamer parameters depend on the electrode polarity. The value of the electric field in the positive streamer channel ($E_{ch} \approx 4$–$5\,\mathrm{kV\,cm^{-1}}$) obtained in [14] corresponds to stationary streamer propagation with constant velocity and agrees with experimental data (reviewed in [15]). For negative streamers, this field is about two to three times greater, in agreement with observation (see [16]) and theoretical investigations [14]. The electron density behind the streamer front is $n_{ch} = 10^{13}$–$10^{14}\,\mathrm{cm^{-3}}$. The diameter of the streamer is of the order of 100–200 μm. In further simulations, we refer to the field in the streamer channel as the external field.

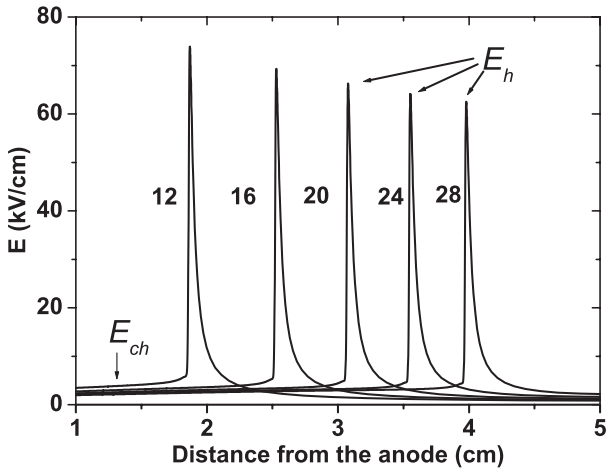

Figure 1. Positive (cathode-directed) streamer development in atmospheric air in a sphere–plane gap (the sphere radius is 0.05 cm and the applied voltage is 5 kV). Profiles of absolute value of the electric field at the streamer axis at five successive time moments are presented. Numbers near the lines denote the time in nanoseconds.

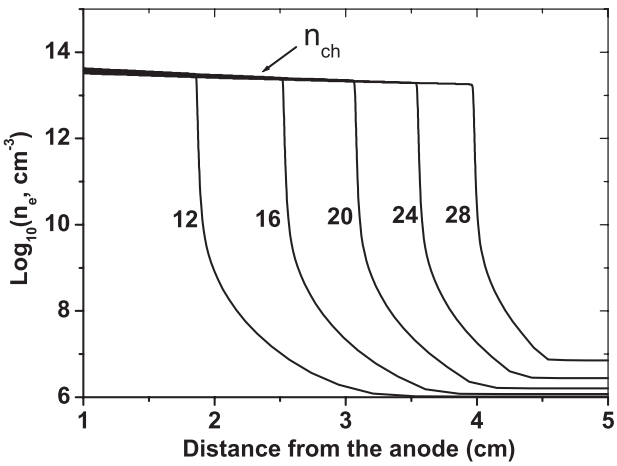

Figure 2. Profiles of electron number density at the streamer axis at five successive time moments. Notation is as in figure 1.

3. Basic equations

In this study, we consider the charging of a spherical conducting dust grain of radius $a = 10\,\mu$m located at the origin of a spherical system of coordinates (see figure 3). We take the direction of initially uniform external electric field as the polar direction (z-axis). The external field is determined by the magnitude of the electric field in the streamer channel ($E_{ext} = E_{ch}$). The system of equations describing the process of the grain charging in two-dimensional spherical coordinates includes the continuity equations for densities of electrons (n_e), positive (n_p) and negative (n_n) ions:

$$\frac{\partial n_e}{\partial t} + \frac{1}{r^2}\frac{\partial}{\partial r}(r^2 j_{er}) + \frac{1}{r\sin\theta}\frac{\partial}{\partial\theta}(\sin\theta\, j_{e\vartheta}) = (\alpha - \eta_2 - \eta_3)V_e n_e - \beta_{ei} n_e n_p + \nu_{detach} n_n, \quad (1)$$

$$\frac{\partial n_p}{\partial t} + \frac{1}{r^2}\frac{\partial}{\partial r}(r^2 j_{pr}) + \frac{1}{r\sin\theta}\frac{\partial}{\partial\theta}(\sin\theta\, j_{p\vartheta}) = \alpha V_e n_e - \beta_{ei} n_e n_p - \beta_{ii} n_n n_p, \quad (2)$$

$$\frac{\partial n_n}{\partial t} + \frac{1}{r^2}\frac{\partial}{\partial r}(r^2 j_{nr}) + \frac{1}{r\sin\theta}\frac{\partial}{\partial\theta}(\sin\theta\, j_{n\vartheta}) = (\eta_2 + \eta_3)V_e n_e - \beta_{ii} n_p n_n - \nu_{detach} n_n. \quad (3)$$

Here, r is the magnitude of the radius vector from the origin and θ is the polar angle; α, η_2 and η_3 are the ionization and two- and three-body attachment coefficients; β_{ei} and β_{ii} are the electron–ion and ion–ion recombination coefficients, correspondingly. The right-hand side of the equations represents the sum of contributions of kinetic processes as sources of particles. The flux densities of the electrons, positive ions and negative ions have the form

$$\boldsymbol{j}_i = n_i \boldsymbol{V}_i - D_i \nabla n_i, \qquad (i = \mathrm{e}, \mathrm{p}, \mathrm{n}), \quad (4)$$

where $\boldsymbol{V}_i$ and D_i denote the drift velocities and the diffusion coefficients.

The system of the continuity equations for all the components is closed by Poisson's equation for the

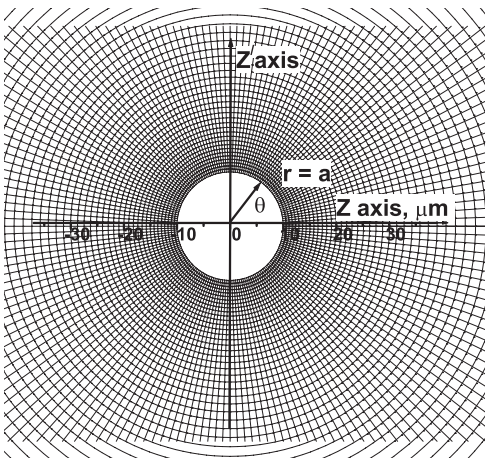

Figure 3. Spherical axisymmetrical mesh.

potential, U,

$$\frac{1}{r^2}\frac{\partial}{\partial r}\left(r^2\frac{\partial U}{\partial r}\right)+\frac{1}{r^2\sin\theta}\frac{\partial}{\partial\theta}\left(\sin\theta\frac{\partial U}{\partial\theta}\right)=-\frac{\rho}{\varepsilon_0}, \qquad (5)$$

where $\rho = e(n_\mathrm{p} - n_\mathrm{n} - n_\mathrm{e})$ is the space charge density. The change in the charge imparted to the grain is given by the following equation:

$$\frac{\mathrm{d}Q}{\mathrm{d}t} = e\int_S(\boldsymbol{\Gamma}_\mathrm{p} - \boldsymbol{\Gamma}_\mathrm{e} - \boldsymbol{\Gamma}_\mathrm{n})\boldsymbol{n}_\mathrm{s}\,\mathrm{d}S, \qquad (6)$$

where $\boldsymbol{n}_\mathrm{s}$ is the unit vector directed towards the particle surface, $\mathrm{d}S = 2\pi a^2\sin\theta\,\mathrm{d}\theta$ is the surface element and e is the absolute value of the electron charge. The fluxes $\boldsymbol{\Gamma}_i$ ($i = \mathrm{e}, \mathrm{p}, \mathrm{n}$) are calculated as follows:

$$\boldsymbol{\Gamma}_i = s_i n_i \boldsymbol{V}_i - D_\mathrm{i}\nabla n_i, \qquad (i = \mathrm{e}, \mathrm{p}, \mathrm{n}). \qquad (7)$$

The symbol s_i is non-zero only if the drift velocity is directed towards the dust grain surface ($s_i = 1$ when the product $\boldsymbol{V}_i\boldsymbol{n}_\mathrm{s}$ is positive and $s_i = 0$ in the opposite case). As drift velocities are field dependent, the fluxes at any point of the surface strongly depend on the polar angle, θ. The first term on the right-hand side of equation (7) represents the so-called field (drift) charging, when the grain is charged by electrons or ions moving in an orderly direction in an external electric field. The second term is the diffusion charging. The transport of charged particles to the surface of a dust grain is considered in the drift–diffusion approximation, which is valid under the condition that the electron and ion mean free paths are much shorter than the characteristic dimension of the problem [17, 18]. For atmospheric air pressure, this condition holds for both electrons and ions.

As the initial conditions, we assume that the uncharged dust grain is immersed in plasma ($n_\mathrm{e} = n_\mathrm{p} = 10^{13}\,\mathrm{cm}^{-3}$) behind the streamer front. The electron and ion density at $r = a$ is zero, and for the outer boundary the number density of charged particles is determined by the processes in the bulk plasma not disturbed by the presence of a dust grain.

Equations (1)–(7) are solved numerically on the non-uniform mesh, which smoothly expands towards the outer boundary (figure 3). The solution of the transport equations is performed by the time-splitting method. A modified flux-corrected transport technique [19, 20] that has small numerical diffusion is used for solving the transport equations in the r and θ directions successively on the non-uniform mesh. The time step is determined by the condition of stability and accuracy [21]. The high order method is used for calculation of the ionization term to obtain a stable solution at high values of the electric field. Poisson's equation is solved using the successive over-relaxation method with the optimum value of the acceleration parameter, ω [22].

4. Elementary processes in the streamer channel in air

In this section, the data on rate constants of elementary processes that are used in our calculations are presented. Plasma parameters in the streamer channel are determined by a set of kinetic processes such as ionization, attachment, detachment and electron–ion and ion–ion recombination. For a not very high concentration of dust grains in the plasma, the electron energy distribution function (EEDF) in a dusty plasma is close (at the values of reduced electric field typical for streamer propagation) to the EEDF in air (see [23]). In our model, the rate constants of reactions including electrons are functions of the reduced field, E/n, and the data for air are used (see [24–28] and references therein).

4.1. Transport coefficients

The electron swarm data [26] are utilized for the following approximation of the drift velocity for electrons:

$$V_\mathrm{e} = 3.2\times10^5\left(\frac{E}{n}\right)^{0.8} \qquad \left(\mathrm{cm\,s^{-1}},\ \frac{E}{n}\ \text{is in Td},\ 1\,\mathrm{Td} = 10^{-17}\,\mathrm{V\,cm^2}\right) \qquad (8)$$

and for ions,

$$V_\mathrm{p,n} = 5.5\times10^2\frac{E}{n} \quad \left(\mathrm{cm\,s^{-1}},\ \frac{E}{n}\ \text{is in Td}\right). \qquad (9)$$

The diffusion coefficients for electrons for atmospheric air pressure are assumed to be equal in both the longitudinal and transverse directions and approximated by the following equation at a gas temperature of 293 K:

$$D_\mathrm{e} = 7\times10^2 + 8\times\left(\frac{E}{n}\right)^{0.8} \quad \left(\mathrm{cm^2\,s^{-1}},\ \frac{E}{n}\ \text{is in Td}\right). \qquad (10)$$

4.2. Diffusion for positive and negative ions

The diffusion coefficient for positive ($i = \mathrm{p}$) and negative ($i = \mathrm{n}$) ions is defined via the Einstein relation,

$$\frac{D_i}{\mu_i} = k_\mathrm{B}\frac{T_i}{e}, \qquad (11)$$

where T_i is the ion temperature, which depends on E/n. T_i can be evaluated according to the Wannier formula [29] (see also [25]),

$$T_i = T_\mathrm{g} + \tfrac{1}{3}(m_i + m)V_i^2. \qquad (12)$$

Here, m_i and m are the masses of the ion and the molecule, V_i is the drift velocity of the ion for a given E/n and T_g is the gas temperature.

4.3. Ionization

The value of the electron-impact ionization coefficient, α/n, is approximated by the expression [27]

$$\frac{\alpha}{n} = \left(1+\frac{6\times10^6}{(E/n)^3}\right)5\times10^{-16}\exp\left(-\frac{1010}{E/n}\right) \qquad \left(\mathrm{cm^2},\ \frac{E}{n}\ \text{is in Td}\right). \qquad (13)$$

4.4. Recombination

Ions and electrons may experience recombination. At pressures of about 1 atm, the ion–ion recombination coefficient depends weakly on the pressure. Its value in air is [30]

$$\beta_{ii} = 2 \times 10^{-6} \left(\frac{300}{T_i}\right)^{1.5}, \quad (\mathrm{cm^{-3}\,s^{-1}}), \tag{14}$$

where T_i can be evaluated according to formula (12). The main process of electron and positive ion recombination in molecular plasma is a dissociative recombination. The rate of electron–ion recombination depends on the sort of ion and on the electric field. At typical streamer channel values of $E = 3$–$10\,\mathrm{kV\,cm^{-1}}$ the electron–ion recombination coefficient for simple ions (N_2^+, O_2^+, NO^+) is $\beta_{ei} = (3\text{–}6) \times 10^{-8}\,\mathrm{cm^3\,s^{-1}}$, and for complex ions ($N_4^+$, O_4^+, $N_2O_2^+$), $\beta_{ei} = (2\text{–}4) \times 10^{-7}\,\mathrm{cm^3\,s^{-1}}$ [25]. Experimental data in molecular nitrogen (possibly with small amount of oxygen) at pressures of about 1 atm give for this interval of E/n the values $\beta_{ei} = (3\text{–}5) \times 10^{-8}\,\mathrm{cm^3\,s^{-1}}$, typical for simple ions. In our calculations for air, the value $\beta_{ei} = 5 \times 10^{-8}\,\mathrm{cm^3\,s^{-1}}$ is used [31].

4.5. Electron attachment

Molecules like O_2 in air have a very strong attachment. This process influence the characteristics of dust grain charging because it limits the mobility of negative charge carriers. Due to the essential role of attachment processes, we treat them in detail. Two types of attachment are taken into account—three- and two-body attachment.

4.5.1. Three-body attachment. In rather weak fields (in the streamer channel), the process of three-body attachment,

$$e + O_2 + O_2 \rightarrow O_2^- + O_2, \tag{15}$$

$$e + O_2 + N_2 \rightarrow O_2^- + N_2, \tag{16}$$

is essential. According to [32, 33], the constants of reactions (15) and (16) are related as 1 : 0.02. Thus, in reaction (15), O_2 molecules are an order of magnitude more effective than N_2 molecules. In this paper, for the three-body attachment coefficient, η_3/n^2, the following approximation is used in the form of an explicit dependence on E/n [25].

$$\frac{\eta_3}{n^2} = 1.6 \times 10^{-37} \left(\frac{E}{n}\right)^{-1.1} \quad \left(\mathrm{cm^5}, \frac{E}{n} \text{ is in Td}\right). \tag{17}$$

The formula (17) overestimates the attachment coefficient for low and zero external fields. In [34], an approximation of experimental data gives the following expressions for the corresponding attachment rate coefficient:

$$K_{att3} = 1.4 \times 10^{-29} \times \frac{300}{T_e} \exp\left(-\frac{600}{T_g}\right) \times \exp\left(\frac{700 \times (T_e - T_g)}{T_e \times T_g}\right) \quad (\mathrm{cm^6\,s^{-1}}). \tag{18}$$

The formula gives the value of the attachment rate $\nu_{att3} \sim 8 \times 10^7\,\mathrm{s^{-1}}$ in zero electric fields (when $T_e \sim T$).

4.5.2. Two-body attachment. For rather high values of electric field ($E > 10$–$15\,\mathrm{kV\,cm^{-1}}$), the reaction of dissociative attachment must be taken into account. In this case, electron-loss processes with formation of negative ions are determined basically by the high-threshold reaction of electron dissociative attachment to oxygen:

$$e + O_2 \rightarrow O^- + O. \tag{19}$$

For the two-body attachment coefficient in air, the most reliable are the data presented in [32], which can be approximated as

$$\frac{\eta_2}{n} = 4.3 \times 10^{-19} \exp\left(-1.05 \left|5.3 - \log_{10}\left(\frac{E}{n}\right)\right|^3\right) \quad (\mathrm{cm^2}). \tag{20}$$

The sum of the two-body attachment and three-body attachment rates (at gas pressure $P = 760\,\mathrm{Torr}$) for air is shown in figure 14 (bottom curve). This value is related to the two-body and three-body attachment coefficients by the expression $\nu_{att} = (\eta_2 + \eta_3) V_e$. Note that the minimum value of the attachment rate is of the order of $10\,\mathrm{kV\,cm^{-1}}$. Also note that in weak fields typical of the streamer channel at atmospheric pressures (3–$10\,\mathrm{kV\,cm^{-1}}$), attachment mainly occurs due to three-body collisions (15).

In figure 4, the absolute value of the difference between the electron attachment and ionization rates, $\nu = (\eta_2 - \eta_3 - \alpha) V_e$, for air at 1 atm is given. This difference is positive for $E < E_{cr}$ and negative for $E > E_{cr}$. The critical value, E_{cr}, of the reduced field at which ionization is equal to the attachment is denoted by the arrow (in air at normal temperature and pressure, the value of E_{cr} is about $25\,\mathrm{kV\,cm^{-1}}$). The electric field in the streamer channel is usually below E_{cr}. Note that in the streamer channel attachment and electron recombination are essential, while the ionization and detachment terms are small. In this case, the ionization cannot maintain the plasma, and the plasma is decaying with the characteristic time $\tau \sim 1/(\eta_2 + \eta_3) V_e$ for an electronegative and $\tau \sim 1/\beta_{ei} n_e$ for an electropositive gas.

4.6. Detachment

The primary ions, O^- and O_2^-, generate a large set of negative ions (O_3^-, O_4^-, NO^-, NO_2^-, NO_3^-) through ion–molecule

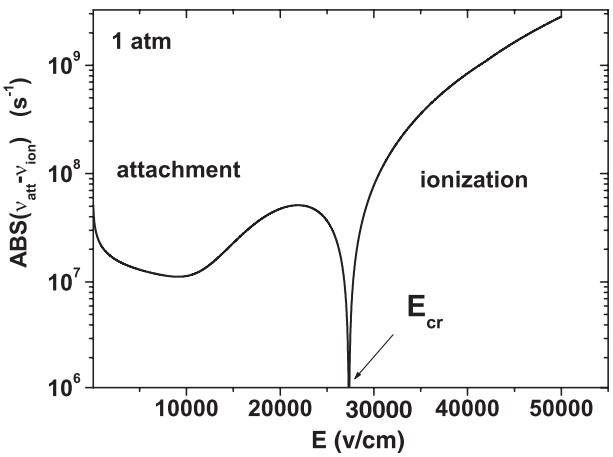

Figure 4. Absolute value of the difference between electron attachment and ionization rates.

association and charge exchange reactions. Since the channels for loss of different sorts of negative ions are different, in order to determine the effective rate at which electrons are removed from negative ions, it is necessary to know the ion composition of the plasma. In this paper, the detachment rate coefficient is used:

$$K_{\text{detach}} = 2 \times 10^{-10} \exp\left(-\frac{6030}{T_i}\right) (\text{cm}^{-3}\,\text{s}^{-1}), \qquad (21)$$

which corresponds to an abundance of O_2^- ions [25], with the effective ion temperature, T_i, calculated according to formula (12).

5. Charging of a dust grain in decaying air and nitrogen plasma (zero external field)

Most experimental work has been conducted for the pulsed regimes of the corona discharge because they are usually more effective. In this section we investigate the process of a particle charging in the decaying air plasma of the streamer trace after a rapid cut-off of the voltage pulse sustaining the discharge (zero external field). The dust grain in air and in nitrogen is charged mainly by electron diffusive fluxes (until the maximum charged is attained) and not by ions. Ion fluxes are essential in the later stages of grain charging. However, the charging process occurs in a different way in attaching (air) and non-attaching (nitrogen) gases. In figure 5, symmetric profiles of plasma charged particles around the dust grain are presented. It is seen that the electron level decreases very rapidly, with the typical time determined mainly by three-body attachment of electrons to O_2 molecules:

$$\tau_{\text{att}} \approx \frac{1}{\nu_{\text{att}}} \approx 10\,\text{ns}. \qquad (22)$$

The characteristic time of the decrease of positive and negative ions is determined by the ion–ion recombination:

$$\tau_{\text{rec}} \approx \frac{1}{\beta_{\text{ii}} n_{\text{p}}} \approx 50\,\text{ns}. \qquad (23)$$

The corresponding electron and ion fluxes to the dust grain are shown in figure 6. Analysis of the fluxes collected by the dust particle shows that the electron diffusive fluxes define the timescale on which the dust particle acquires the maximal charge. The decrease of these fluxes is governed by the attachment rate. The moment when the maximal charge is attained is indicated in figure 6 by the arrow.

It is interesting to compare the evolution of charge collected by the dust grain in decaying plasma in attaching (air) and non-attaching (nitrogen) gases. For nitrogen, the corresponding time of electron decrease is defined by electron–ion recombination; this process is very slow and is of the order of a few microseconds:

$$\tau_{\text{rec}} \approx \frac{1}{\beta_{\text{ei}} n_{\text{e}}} \approx 2\,\mu\text{s}. \qquad (24)$$

In decaying nitrogen plasma, the charging time (when the maximal charge is attained) is comparable with that in a stationary plasma [18]. As a result, the charging time for air is essentially less than that for nitrogen. In figure 7, evolution of electrons and ions around the dust grain in a decaying nitrogen plasma is shown, and figure 8 demonstrates the corresponding electron and ion fluxes. The maximal value of the attained charge is greater in nitrogen plasma compared with that in air, and the charge in both cases exceeds the value of 10^5 electron charges (figure 9). Consideration of further processes of charge neutralization by slow ions is beyond the scope of this paper.

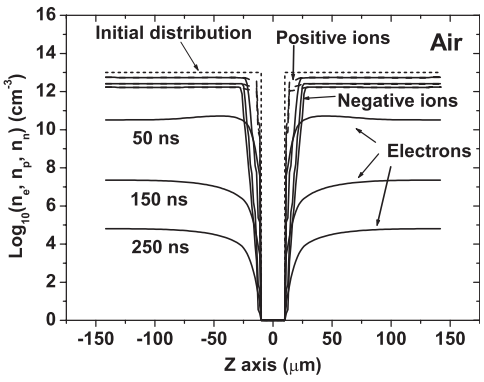

Figure 5. Evolution of electrons and positive and negative ions around the dust grain (along z-axis) during the first 250 ns of the dust grain charging in a decaying air plasma (zero external field). The curves are shown for three successive time moments. The centre of the dust grain is located at $z = 0$.

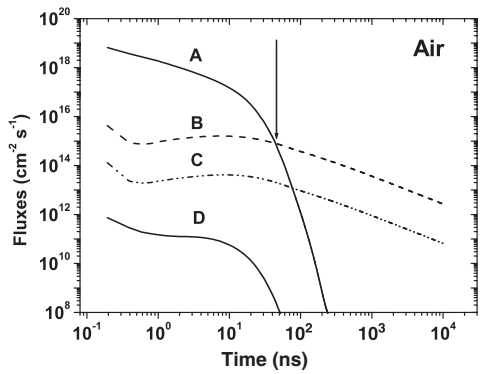

Figure 6. Diffusion and drift fluxes of charged plasma particles collected by the spherical dust grain in decaying plasma (air). Curve A, diffusion flux of electrons; curve B, drift flux of positive ions; curve C, diffusion flux of positive ions; and curve D, diffusion flux of negative ions.

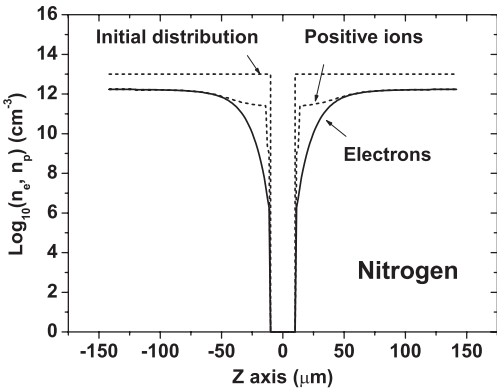

Figure 7. Distribution of electrons and positive ions around the dust grain in decaying nitrogen plasma at 10 000 ns (zero external field). The centre of the dust grain is located at $z = 0$.

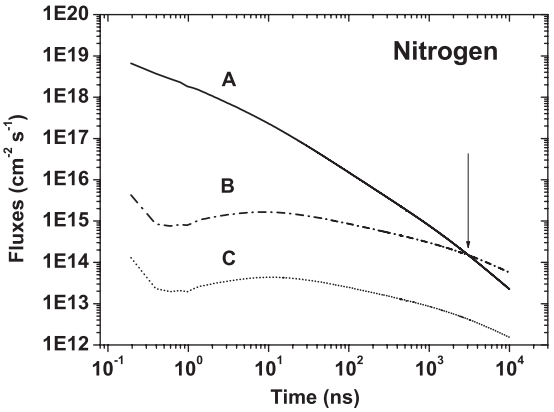

Figure 8. Diffusion and drift fluxes of charged particles collected by the spherical dust grain in decaying plasma (nitrogen). Curve A, diffusion flux of electrons; curve B, drift flux of positive ions; curve C, diffusion flux of positive ions.

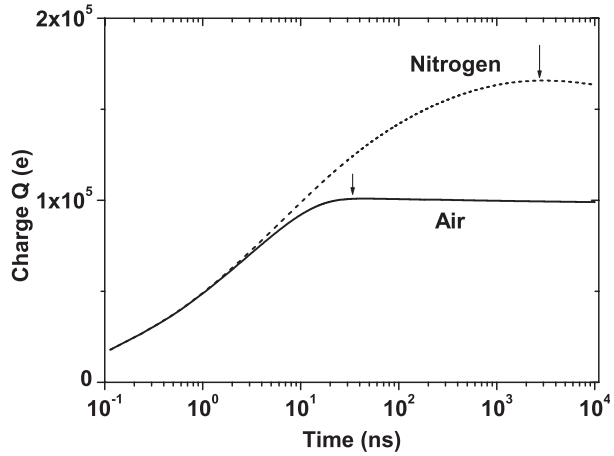

Figure 9. Time evolution of charge accumulated on the dust grain in decaying air and nitrogen plasmas in zero external field. The arrows indicate the moment when the charge attains its maximal value.

Note that the electron diffusive fluxes play the essential role in the process of the dust grain charging in a non-stationary air plasma as they determine the timescale on which the dust particle acquires the maximal charge.

6. Charging of a dust grain in external fields

The problem of a dust grain charging in the streamer channel can be formulated as a charging process in external fields. The absolute values of the electric field in the streamer channel do not exceed $E_{\rm cr}$ (figure 4). Thus, the plasma in the streamer channel is decaying.

The distribution of the electric field around an uncharged conducting sphere (dust grain) placed in an initially uniform electric field, $E_{\rm ext}$, can be obtained analytically [35]. The field lines of a uniform electric field are parallel, but the presence of the conductor alters the field in such a way that the field lines strike the surface of the conductor, which is an equipotential surface, normally. In the process of the dust grain charging, we account for the potential of charges accumulated on its surface and for the potential produced by space charges near the grain. The electric field produced by

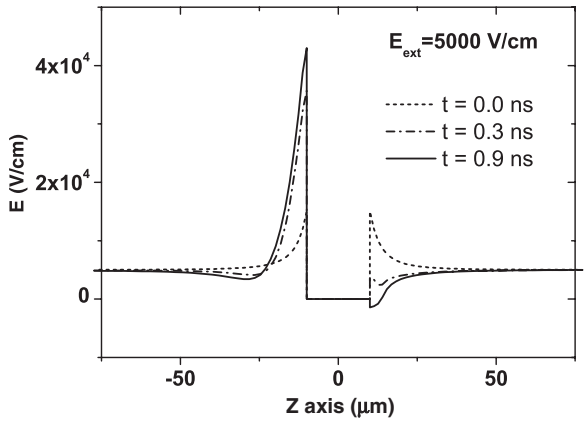

Figure 10. Evolution of the absolute value of the electric field along the z-axis during the initial stage of the charging process. The centre of the dust grain is located at $z = 0$.

accumulated charges is directed towards the surface. Thus, on the left-hand side, this field is added to the external field and, consequently, subtracted on the right-hand side. The total field is the superposition of the external field, the field of the accumulated charges and the field produced by space charges. The very initial stage of electric field redistribution is shown in figure 10. Figures 11(a) and (b) demonstrate the evolution of the potential and electric field after 30 ns of the charging process in an external field, $E_{\rm ext} = 5000\,{\rm V\,cm^{-1}}$. As can be seen, in external fields (in the streamer channel) the charging process occurs in very non-uniform and non-stationary conditions. In this case, the distribution of charged plasma particles and, consequently, drift and diffusion fluxes to the grain surface depend on the polar angle, θ, as indicated in figure 12. Here, we also observe the substantial decrease in electron concentration due to attachment. The decrease in ion level is due to recombination processes. Note that in weak fields typical for the streamer channel at atmospheric pressures, attachment and electron recombination are essential, while ionization and detachment processes are negligible. Attachment occurs mainly due to three-body collisions. In this case, the ionization cannot maintain the plasma, and the plasma density is decreasing with the characteristic time $\tau_{\rm e} \sim 1/(\eta_2 + \eta_3)V_{\rm e}$ for electrons and $\tau_i \sim 1/\beta_{\rm ii}n_{\rm p}$ for ions (the drift velocity, $V_{\rm e}$, depends on the external field). The region in which the quasi-neutrality of the plasma is significantly violated is of the order of 50 μm on the left-hand side of the dust grain ($\theta = \pi$) and is much smaller on its right-hand side ($\theta = 0$), where the grain faces the electron flow. In figure 13, the process of grain charging is shown for different values of external electric field. The arrows mark the moments when the maximal charge is attained. The corresponding charging times correlate with the attachment rate curve (figure 14). These times are large for fields of 8–10 ${\rm kV\,cm^{-1}}$. The indicated values of the electric field correspond to the minimal value of the attachment rates. In this region, three-body attachment is already not efficient, but the electrons do not possess sufficient energy for dissociative (two-body) attachment. Due to the essential role of the mobile electrons in the charging process, the charging time is defined mainly by the attachment process and, consequently, by the level of electron concentration near the particle. As a result,

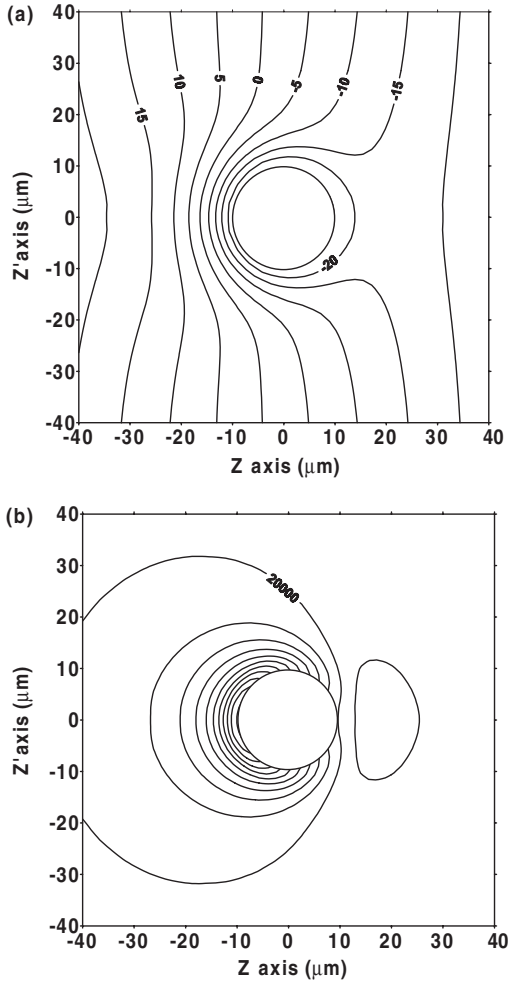

Figure 11. Contours of (*a*) potential and (*b*) absolute value of the electric field around the conducting dust grain after 30 ns of the charging process in the external field, $E_{\text{ext}} = 5000\,\text{V cm}^{-1}$. (The contour lines for the electric field are shown in $4000\,\text{V cm}^{-1}$.)

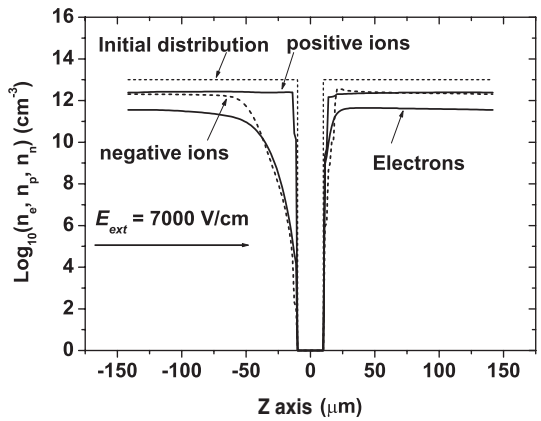

Figure 12. The asymmetric profile of charged particle distribution around the dust grain (along z-axis) after 250 ns charging in an external field of $7000\,\text{V cm}^{-1}$. The direction of the external filed is indicated by the arrow.

for negative streamers ($E_{\text{ch}} \approx 8$–$10\,\text{kV cm}^{-1}$) the time needed for a dust grain to attain the maximal charge (∼200–300 ns) is greater than the corresponding time for positive streamers (∼100 ns).

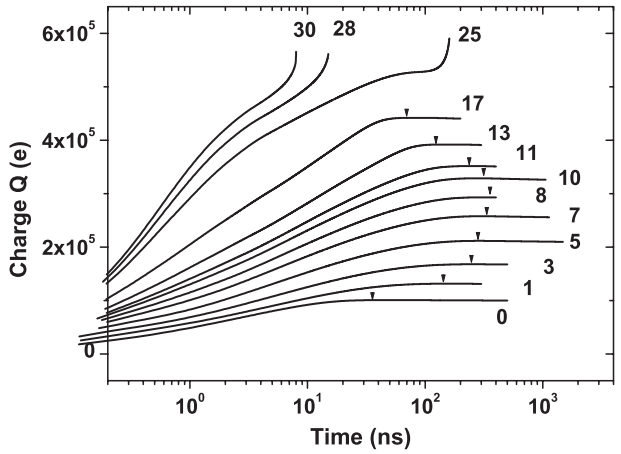

Figure 13. Particle charge as a function of time for the different values of E_{ext} (kV cm^{-1}) that label the curves. The arrows indicate the moment when the grain charge attains its maximal value.

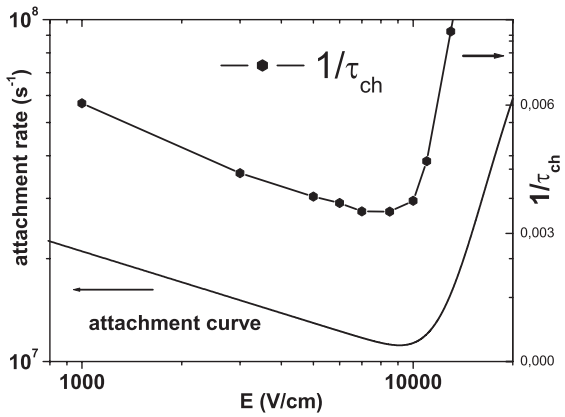

Figure 14. Correlation between the attachment rate curve and charging time, τ_{ch} (time needed for the grain to attain the maximal charge).

For high electric fields, the accumulated charge can be very large and the formation of corona discharge can be observed starting preferably from the left-hand side of the dust grain ($\theta = \pi$), which faces the direction of the external field and where the electric field is higher. The process is analogous to that of Trichel pulse formation in a negative corona [36]. The spatial distribution of the electric field near the dust grain at three successive moments is shown in figure 15 and, with higher resolution (in figure 16). The process is very rapid and develops within 1 ns. A detailed consideration of this process is beyond the scope of this paper.

7. Conclusions

In this paper, we have presented a numerical model of a dust grain charging in decaying plasma of the streamer channel. For a zero external field, it was demonstrated that the process occurs in a different way in attaching (air) and non-attaching (nitrogen) gases. For non-zero external fields, a correlation between the charging time in air and the field dependence of the attachment rate is revealed. For high values of the external fields, a corona discharge starting from the dust grain was observed.

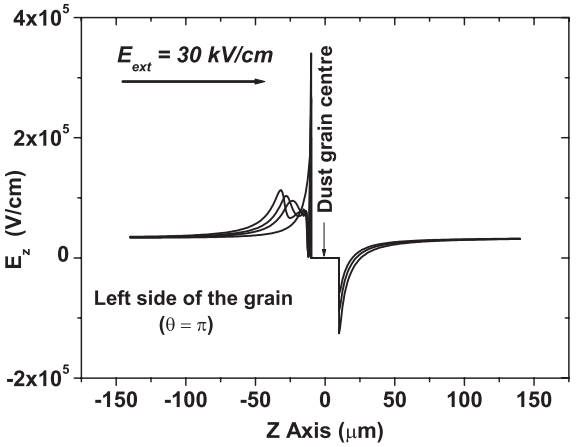

Figure 15. Corona discharge starting from the dust grain. Distribution of the z-component of the electric field at three successive time moments.

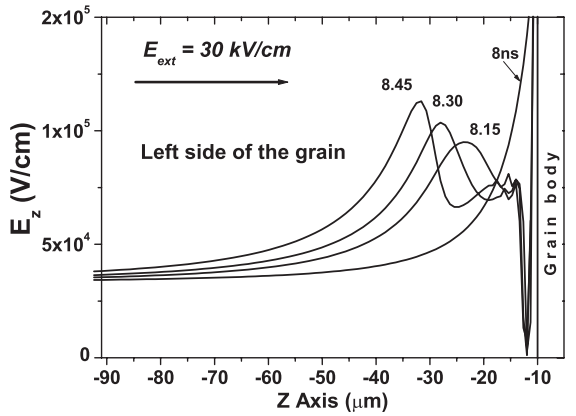

Figure 16. Left-hand side of the dust grain. Magnified from figure 15.

Acknowledgments

Helpful discussions with Professor G V Naidis and Professor M S Benilov are gratefully acknowledged. This study was supported by the Korea Research Foundation Grant (KRF-2000-015-DS0010) and Korea Ministry of Education through its Brain Korea 21 programme.

References

[1] Loeb L B 1965 *Electrical Coronas* (Berkeley, CA: University of California Press)
[2] Meek J M and Craggs J D 1978 *Electrical Breakdown of Gases* (Chichester: Wiley-Interscience)
[3] Veldhuizen E M (ed) 1999 *Electrical Discharges for Environmental Purposes: Fundamentals and Applications* (New York: NOVA Science Publishers)
[4] Shukla P K 2001 *Phys. Plasmas* **8** 1791
[5] Mendis D A 2002 *Plasma Sources Sci. Technol.* **11** A219
[6] Boufendi L and Bouchoule A 2002 *Plasma Sources Sci. Technol.* **11** A211
[7] Fortov V E *et al* 2001 *Phys. Rev. Lett.* **87** 205002
[8] Hur M S, Lee H J and Lee J K 1999 *IEEE Trans. Plasma Sci.* **27** 1449
[9] Choi S J and Kushner M J 1994 *J. Appl. Phys.* **75** 3351
[10] Choi S J and Kushner M J 1994 *IEEE Trans. Plasma Sci.* **22** 138
[11] Reist P C 1993 *Aerosol Science and Technology* (New York: McGraw-Hill)
[12] Dascalescu L, Mihailscu M and Mizuno A 1996 *J. Phys. D: Appl. Phys.* **29** 522
[13] Babaeva N Yu and Naidis G V 1996 *J. Phys. D: Appl. Phys.* **29** 2423
[14] Babaeva N Yu and Naidis G V 1997 *IEEE Trans. Plasma Sci.* **25** 375
[15] Allen N L and Ghaffar A 1995 *J. Phys. D: Appl. Phys.* **28** 331
[16] Raizer Yu P 1991 *Gas Discharge Physics* (Berlin: Springer)
[17] Pal' A F, Starostin A N and Filippov A V 2001 *Plasma Phys. Rep.* **27** 143
[18] Pal' A F, Serov A O, Starostin A N, Filippov A V and Fortov V E 2001 *J. Exp. Theor. Phys.* **92** 235
[19] Morrow R and Cram L E 1985 *J. Comput. Phys.* **57** 129
[20] Kunhardt E E and Wu C 1987 *J. Comput. Phys.* **68** 127
[21] Vitello P A, Penetrante B M and Bardsley J N 1994 *Phys. Rev.* E **49** 5574
[22] Smith G D 1985 *Numerical Solution of Partial Differential Equations* (Oxford: Clarendon)
[23] Ivanov V V, Rakhimova T V, Serov A O, Suetin N V and Pal' A F 1999 *J. Exp. Theor. Phys.* **88** 1105
[24] Yousfi M, Azzi N, Segur P, Gallimberti I and Stangherlin S 1988 Electron–molecule collision cross sections and electron swarm parameters in some atmospheric gases *Report CPAT* (Toulouse: Université Paul Sabatier)
[25] Mnatsakanyan A Kh and Naidis G V 1991 *Reviews of Plasma Chemistry* ed B M Smirnov (New York: Consultants Bureau) p 259
[26] Gallagher J W, Beaty E C, Dutton J and Pitchford L C 1983 *J. Chem. Ref. Data* **12** 109
[27] Gallimberti I 1988 *Pure Appl. Chem.* **60** 663
[28] Aleksandrov N L, Bazelyan E M, Kochetov I V and Dyatko N A 1997 *J. Phys. D: Appl. Phys.* **30** 1616
[29] Wannier G H 1953 *Bell Syst. Tech. J.* **32** 170
[30] Smirnov B M 1982 *Negative Ions* (New York: McGraw-Hill)
[31] Naidis G V 1999 *J. Phys. D: Appl. Phys.* **32** 2649
[32] Pack J L and Phelps A V 1966 *J. Chem. Phys.* **45** 4316
[33] Chanin L M, Phelps A V and Biondi M A 1961 *Phys. Rev.* **128** 219
[34] Kossyi I A, Kostinsky A Yu, Matveyev A A and Silakov V P 1992 *Plasma Sources Sci. Technol.* **1** 207
[35] Reitz J R, Milford F J and Christy R W 1991 *Foundation of Electromagnetic Theory* (Reading, MA: Addison-Wesley)
[36] Napartovich A P, Akishev Yu S, Deryugin A A, Kochetov I V, Pan'kin M V and Trushkin N I 1997 *J. Phys. D: Appl. Phys.* **30** 2726